Nanoscale Hydrophobic Recovery: A Chemical Force Microscopy Study of UV/Ozone-Treated Cross-Linked Poly(dimethylsiloxane)

Henrik Hillborg, Nikodem Tomczak, Attila Olàh,† Holger Schönherr, and G. Julius Vancso*

Faculty of Science and Technology and MESA+ Institute for Nanotechnology, Department of Materials Science and Technology of Polymers, University of Twente, P.O. Box 217, 7500 AE Enschede, The Netherlands

Received August 22, 2003. In Final Form: November 25, 2003

Chemical force microscopy (CFM) in water was used to map the surface hydrophobicity of UV/ozone-treated poly(dimethylsiloxane) (PDMS; Sylgard 184) as a function of the storage/recovery time. In addition to CFM pull-off force mapping, we applied indentation mapping to probe the changes in the normalized modulus. These experiments were complemented by results on surface properties assessed on the micrometer scale by X-ray photoelectron spectroscopy and water contact-angle measurements. Exposure times of ≤30 min resulted in laterally homogeneously oxidized surfaces, which are characterized by an increased modulus and a high segmental mobility of PDMS. As detected on a sub-50-nm level, the subsequent "hydrophobic recovery" was characterized by a gradual increase in the pull-off forces and a decrease in the normalized modulus, approaching the values of unexposed PDMS after 8−50 days. Lateral imaging on briefly exposed PDMS showed the appearance of liquid PDMS in the form of droplets with an increasing recovery time. Longer exposure times (60 min) led to the formation of a hydrophilic silica-like surface layer. Under these conditions, a gradual surface reconstruction within the silica-like layer occurred with time after exposure, where a hydrophilic SiO_x-enriched phase formed <100-nm-sized domains, surrounded by a more hydrophobic matrix with lower normalized modulus. These results provide new insights into the lateral homogeneity of oxidized PDMS with a resolution in the sub-50-nm range.

Introduction

The recent advances in microfluidic devices and soft lithography have opened up new areas of application of cross-linked poly(dimethylsiloxane) (PDMS).[1] Soft lithography is a collective name of a number of lithographic methods, which often utilize inked PDMS stamps with patterned relief structures to generate structures with feature sizes down to ∼100 nm.[2] The low surface tension of PDMS (21−23 mJ m^{-2})[3] is a result of closely packed methyl groups at the surface.[4] In many soft lithography applications, the intrinsic hydrophobic surface properties are sufficient, whereas in other cases the hydrophobicity has to be reduced to obtain the desired results, for example, when using hydrophilic inks or by the direct stamping of proteins.[5] In microfluidic applications, a reduction of the hydrophobicity of PDMS improves the wettability of aqueous solutions and reduces nucleation of air bubbles in the microchannels.[5b]

Reduction of the hydrophobicity can be achieved by exposing PDMS to different types of oxidizing plasmas,[6] corona discharges,[6b,7] or UV radiation.[8] The oxidation process within the top 10 nm of the surface has been extensively investigated using X-ray photoelectron spectroscopy (XPS). It was found that the atomic content of carbon decreases and the content of oxygen increases, whereas the silicon content remains essentially unchanged.[6−8] Moreover, the binding energy of the Si(2p) photoelectrons shifts toward the value characteristic for inorganic silica (SiO_2, ∼103.5 eV), indicating the formation of a silica-like layer (SiO_x).[6b−f,7,8a,c] The oxidation rate is initially rapid, but decreases considerably with increasing

† Dutch Polymer Institute (DPI), P.O. Box 217, 7500 AE Enschede, The Netherlands.

* Corresponding author. Tel.: +31-53-4892967. Fax: +31-53-4893823. E-mail address: g.j.vancso@utwente.nl.

(1) (a) Duffy. D. C.; McDonald. J. C.; Schueller, J. A.; Whitesides, G. M. *Anal. Chem.* **1998**, *70*, 4974. (b) McDonald, J. C.; Duffy, D. C.; Anderson, J. R.; Chiu, D. T.; Wu, H.; Schueller, O. J. A.; Whitesides, G. M. *Electrophoresis* **2000**, *21*, 27. (c) Hu, S.; Ren, X.; Bachman, M.; Sims, C. E.; Li, G. P.; Allbritton, N. *Anal. Chem.* **2002**, *74*, 4117. (d) Ro, K. W.; Lim, K.; Kim, H.; Hahn, J. H. *Electrophoresis* **2002**, *23*, 1129.

(2) (a) For a review, see Xia, Y.; Whitesides, G. M. *Angew. Chem., Int. Ed.* **1998**, *37*, 550. (b) Xia, Y.; Rogers, J. A.; Paul, K. E.; Whitesides, G. M. *Chem. Rev.* **1999**, *99*, 1823. (c) Jackman, R. J.; Wilbur, J. L.; Whitesides, G. M. *Science* **1995**, *264*, 664. (d) Schmid, H.; Michel, B.; *Macromolecules* **2000**, *33*, 3042. (e) Donzel, C.; Geissler, M.; Bernard, A.; Wolf, H.; Michel, B.; Hilborn, J.; Delamarche, E. *Adv. Mater.* **2001**, *13*, 1164. (f) Odom, T. W.; Love, J. C.; Wolfe, D. B.; Paul, K. E.; Whitesides, G. M. *Langmuir* **2002**, *18*, 5314.

(3) Owen, M. J. *Ind. Eng. Chem. Prod. Res. Dev.* **1980**, *19*, 97.

(4) Owen, M. J. In *Silicon-Based Polymer Science, A Comprehensive Resource*; Ziegler, J., Fearon, F. W. G., Eds.; Advances in Chemistry Series 224; American Chemical Society: Washington, DC, 1990.

(5) (a) Bernard, A.; Delamarche, E.; Schmid, H.; Michel, B.; Bosshard, H. R.; Biebuyck, H. *Langmuir* **1998**, *14*, 2225. (b) Martin, B. D.; Brandow, S. L.; Dressick, W. J.; Schull, T. L. *Langmuir* **2000**, *16*, 9944.

(6) (a) Morra, M.; Occhiello, E.; Marola, R.; Garbassi, F.; Humphrey, P.; Johnson, D. *J. Colloid Interface Sci.* **1990**, *137*, 11. (b) Tóth, A.; Bertóti, I.; Blazló, M.; Bánhegyi, G.; Bognar, A.; Szaplonczay, P. *J. Appl. Polym. Sci.* **1994**, *52*, 1293. (c) Owen, M. J.; Smith, P. J. *J. Adhes. Sci. Technol.* **1994**, *8*, 1063. (d) Fritz, J.; Owen, M. J. *J. Adhes.* **1995**, *54*, 33. (e) Hillborg, H.; Ankner, J. F.; Gedde, U. W.; Smith, G. D.; Yasuda, H. K.; Wikström, K. *Polymer* **2000**, *41*, 6851. (f) Hillborg, H.; Sandelin, M.; Gedde, U. W. *Polymer* **2001**, *42*, 7349. (g) Chua, D. B. H.; Ng, H. T.; Li, S. F. Y. *Appl. Phys. Lett.* **2000**, *76*, 721.

(7) Hillborg, H.; Gedde, U. W. *Polymer* **1998**, *39*, 1991.

(8) (a) Mirley, C. L.; Koberstein, J. T. *Langmuir* **1995**, *11*, 1049. (b) Vasilets, V. N.; Nakamura, K.; Uyama, Y.; Ogata, S.; Ikada, Y. *Polymer* **1997**, *39*, 2875. (c) Ouyang, M.; Yuan, C.; Muisener, R. J.; Boulares, A.; Koberstein, J. T. *Chem. Mater.* **2000**, *12*, 1591. (d) Phely-Bobin, T. S.; Muisener, R. J.; Koberstein, J. T.; Papadimitrakopoulos, F. *Adv. Mater.* **2000**, *12*, 1257.

10.1021/la035552k CCC: $27.50
Published on Web 12/30/2003

exposure times.[6e,f,8a,c,9] To explain the SiO_x formation on PDMS surfaces, a model was developed, which proposes two different regions of growth-rate behavior.[8a,9] The first region, exhibiting a high oxidation rate, involves the removal of carbon in the form of volatile species and oxidative cross-linking via Si−O bridges, leading to the gradual formation of a continuous barrier layer of SiO_x. The second region, exhibiting a low oxidation rate, occurs after the formation of an effective SiO_x barrier, where the diffusion of oxidative species into the PDMS network becomes the rate-limiting step. The lifetime of these reactive species limits the thickness of the oxidized layer. The thickness of the SiO_x layer formed after plasma or UV treatments ranges between 7 and 160 nm.[6c,e,8a,c] The difference in the reported layer thicknesses may be due to the difference in the oxidation conditions or due to the different information depths of the analytical methods utilized to assess the thickness.

During the last few years, a number of potential applications of these silica-like layers have been discussed in the literature. As a result of the large difference in the thermal expansion coefficient between the SiO_x−surface layer and the underlying PDMS, spontaneous formation of complex structures on oxygen−plasma-treated PDMS has been observed, which could be extended to the fabrication of ordered patterns.[6g] Spontaneous formation of regular patterns in thin gold films deposited on PDMS, previously photopatterned using UV radiation, has been described by Huck et al.[10] Because the SiO_x layers exhibit a high resistance to oxygen and water together with a high gas selectivity, this may lead to their use as moisture barriers, protective layers, or gas-separation membranes.[8c,11]

The hydrophobicity recovers, however, partially or fully with time after exposure.[6a−f,7] The phenomenon restricts the usefulness of plasma oxidation of PDMS stamps for soft lithography.[2e] Similarly, a difficulty with the use of oxidized PDMS microchannels is the instability of the aqueous fluid flow upon exposure of the PDMS devices to air, caused by the hydrophobic recovery.[1b,c] The recovery process has been extensively investigated and can be explained as follows:[6,7,12] Free low-molar-mass PDMS chains, either formed by chain scission reactions during the oxidation or intrinsically present as residues from the polymerization or cross-linking reactions, migrate to the surface through a porous or cracked hydrophilic silica-like layer. To reduce the free surface energy, these species gradually cover the surface, resulting in a recovery of hydrophobicity. The rate of this hydrophobic recovery is influenced by the morphology of the surface layer. If cracking of the silica-like layer can be induced, the rate of hydrophobic recovery increases as a result of a faster migration of low molar mass siloxanes to the surface.[6c−f]

Stiffness changes of plasma-oxidized PDMS were recently characterized using tapping-mode scanning force microscopy (SFM).[13] The stiffness of the surface initially increased and thereafter remained essentially constant with increasing exposure time. Moreover, it was observed that the surface stiffness remained unchanged with the recovery time after exposure, even though the surface exhibited a hydrophobic recovery as assessed by water contact-angle measurements, thus supporting the diffusion mechanism.[14]

Another mechanism contributing to the hydrophobic recovery is reorientation of polar groups from the surface to the bulk or reorientation of nonpolar groups from the bulk to the surface.[6a,c,d,15] It has been suggested that by using mild oxidation conditions, in which only a few of the polymer side groups are oxidized, this mechanism is important for the recovery. This process, however, decreases in significance during the formation of the silica-like phase, which prevents reorientation from occuring, while the diffusion-controlled migration of free siloxanes becomes the dominant process.[6c−f,12]

To gain further understanding of these processes, it is important to investigate and understand the lateral homogeneity of these silica-like layers on a submicrometer scale. On the basis of this knowledge, new ways to characterize and control local variations in hydrophobicity, improve printability and wettability on the micrometer scale, or inhibit the formation of cracks and pores in SiO_x layers for improved barrier properties could be developed. Chemical force microscopy (CFM) is a scanning probe technique that combines chemical discrimination with the high spatial resolution of SFM by exploiting the forces between chemically derivatized scanning probe tips and the surface.[16] In the originally introduced approach,[17] various terminal functional groups in self-assembled monolayers on gold were differentiated in pull-off and friction force measurements.[18] In many cases, normal and lateral forces show similar relative contrast; however, exceptions have been reported.[19] These exceptions are related to contributions of energy dissipation in disordered organic systems[20] or orientation effects[21] to the friction forces measured. Even though the mapping of pull-off forces[22] is slow compared to friction imaging,[23] pull-off force measurements are often more straightforward to interpret.[24] The pull-off forces depend systematically on

(9) Chan, V. Z. H.; Thomas, E. L.; Frommer, J.; Sampson, D.; Campbell, R.; Miller, D.; Hawker, C.; Lee, V.; Miller, R. D. *Chem. Mater.* **1998**, *10*, 3895.

(10) Huck, W. T. S.; Bowden, N.; Onck, P.; Pardoen, T.; Hutchinson, J. W.; Whitesides, G. M. *Langmuir* **2000**, *16*, 3497.

(11) Ouyang, M.; Yuan, C.; Muisener, R. J.; Boulares, A.; Koberstein, J. T. *J. Membr. Sci.* **2000**, *177*, 177.

(12) Kim, J.; Chaudhury, M. K.; Owen, M. J. *J. Colloid Interface Sci.* **2000**, *226*, 231.

(13) Bar, G.; Delineau, L.; Häfele, A.; Whangbo, M. H. *Polymer* **2001**, *42*, 3627.

(14) The probed depths ranged between 10 and 60 nm, significantly higher than the probed depth in this study, <10 nm.

(15) Yasuda, H. K.; Sharma, A. K.; Yasuda, T. *J. Polym. Sci., Part B: Polym. Phys.* **1981**, *19*, 1265.

(16) Frisbie, C. D.; Rozsnyai, L. F.; Noy, A.; Wrighton, M. S.; Lieber, C. M. *Science* **1994**, *265*, 2071.

(17) For a review, see Noy, A.; Vezenov, D. V.; Lieber, C. M. *Annu. Rev. Mater. Sci.* **1997**, *27*, 381.

(18) (a) Sinniah, S. K.; Steel, A. B.; Miller, C. J.; Reutt-Robey, J. E. *J. Am. Chem. Soc.* **1996**, *118*, 8925. (b) Vezenov, D. V.; Noy, A.; Rozsnyai, L. F.; Lieber, C. M. *J. Am. Chem. Soc.* **1997**, *119*, 2006. (c) van der Vegte, E. W.; Hadziioannou, G. *Langmuir* **1997**, *13*, 4357. (d) van der Vegte, E. W.; Hadziioannou, G. *J. Phys. Chem. B* **1997**, *101*, 9563. (e) McKendry, R.; Theoclitou, M. E.; Rayment, T.; Abbell, C. *Nature* **1998**, *391*, 566.

(19) For an example, see Jenkins, A. T. A.; Boden, N.; Bushby, R. J.; Evans, S. D.; Knowles, P. F.; Miles, R. E.; Ogier, S. D.; Schönherr, H.; Vancso, G. J. *J. Am. Chem. Soc.* **1999**, *121*, 5274.

(20) (a) Xiao, X.; Hu, J.; Charych, D. H.; Salmeron, M. *Langmuir* **1996**, *12*, 235. (b) Lio, A.; Charych, D. H.; Salmeron, M. *J. Phys. Chem. B* **1997**, *101*, 3800.

(21) (a) Vancso, G. J.; Schönherr, H. In *Microstructure and Microtribology of Polymer Surfaces*; Tsukruk, V. V., Wahl, K. J., Eds.; ACS Symposium Series 741; American Chemical Society: Washington, DC, 2000; Chapter 19, pp 317−335. (b) Schönherr, H.; Kenis, P. J. A.; van Hummel, G. J.; Harkema, S.; Hulst, R.; Engbersen, J. F. J.; Reinhoudt, D. N.; Vancso, G. J. *Langmuir* **1998**, *14*, 2801.

(22) (a) Joyce, S. A.; Houston, J. E.; Michalske, T. A. *Appl. Phys. Lett.* **1992**, *60*, 1175. (b) van der Werf, K. O.; Putman, C. A. J.; de Grooth, B. G.; Greve, J. *Appl. Phys. Lett.* **1994**, *65*, 1195. (c) Baselt, D. R.; Baldeschwieler, J. D. *J. Appl. Phys.* **1994**, *76*, 33. (d) Radmacher, M.; Cleveland, J. P.; Fritz, M.; Hansma, H. G.; Hansma, P. K. *Biophys. J.* **1994**, *66*, 2159. (e) Berger, C. E. H.; van der Werf, K. O.; Kooyman, R. P. H.; de Grooth, B. G.; Greve, J. *Langmuir* **1995**, *11*, 4188.

(23) Carpick, R. W.; Salmeron, M. *Chem. Rev.* **1997**, *97*, 1163.

(24) Schönherr, H. Ph.D. Thesis, University of Twente, Enschede, The Netherlands, 1999.

various factors, such as tip functionality and liquid medium, and can be rationalized on the basis of surface free energy considerations and solvent exclusion arguments.[18a,25] For apolar polymers, Feldmann et al. showed that the Lifshitz−van der Waals theory can be utilized to rationalize the corresponding interactions and that the dispersive interactions can be amplified by using perfluorodecaline as the medium for force measurements to enable one to differentiate different polymers.[26] The general strategy of CFM can be extended to polymers containing polar functional groups[27] and elastomers, including PDMS,[28] as previously shown in our group. In particular, laterally resolved force−volume (FV) measurements as a function of the pH allowed us to obtain maps of functional group distributions in surface-treated and functional polymers with sub-50-nm resolution.[29]

In this paper, we present the first systematic study that addresses the oxidation of PDMS surfaces and the concomitant hydrophobic recovery from a nanometer-scale perspective. Using CFM, we mapped the surface hydrophobicity of silica-like surface layers on UV/ozone-treated PDMS and followed their changes as a function of the storage/recovery time after exposure. In addition to CFM pull-off force mapping, we applied indentation mapping to probe the changes in the normalized modulus. These experiments were complemented by results on surface properties assessed on the micrometer scale by XPS and water contact-angle measurements. To our knowledge, the application of laterally resolved adhesion imaging on silica-like surface layers on oxidized PDMS has not been previously reported.

Experimental Section

Sample Preparation. Sylgard 184 (Dow Corning), consisting of PDMS and a reinforcing silica filler, was prepared by carefully mixing the precursors Sylgard 184A/Sylgard 184B at a ratio of 10:1 by mass.[30] The mixture was subsequently degassed in a vacuum oven at room temperature. Glass cover slides or silicon substrates were cleaned using Piranha solution (mixture of 1:4 of 30% H_2O_2 and concentrated H_2SO_4), carefully rinsed several times in Milli-Q water and ethanol, and finally dried in a stream of nitrogen gas. *Caution! Piranha solution is a very strong oxidant, reacts violently with organic materials, and should be handled with the utmost care!* The PDMS was spin-coated onto the substrates using a Spincoater model P6700 (Specialty Coating Systems, Inc.). After spin coating, the films were cured at 120 °C overnight and stored individually in plastic containers. The thickness of the PDMS films was 830 ± 100 nm according to ellipsometry (a Plasmos SD 2002 ellipsometer was used at a wavelength of 632.8 nm and a fixed incident angle of 70°; n_f was assumed to be 1.4). The thickness was determined on at least nine different locations of each film.

UV/Ozone Treatment. The UV/ozone treatment of the PDMS surfaces was performed in a commercial UV/ozone cleaner (Ultra-Violet Products PR-100). The apparatus contains a low-pressure mercury UV light, generating UV emissions at 185 nm (1.5 mW cm^{-2}) and 254 nm (15 mW cm^{-2}). The distance between the UV source and the PDMS films was 20 mm. The nominal ozone steady-state concentration of 55 ppm was produced in a two-step photochemical process initiated by the photolysis of molecular oxygen at 185 nm. The ozone is then photodecomposed by absorption of UV radiation at 254 nm, resulting in the formation of atomic oxygen. Organic molecules react further with the atomic oxygen, forming volatile molecules, which then desorb from the exposed surface.

Contact-Angle Measurements. The advancing and receding contact angles (θ_a and θ_r) were measured with Millipore water (18.4 MΩ cm) as a probe liquid by using a contact-angle microscope (Data Physics, OCA 15plus) and the sessile drop method.[31] The advancing and receding contact angles were measured on both sides of the drop and on at least three different locations on each sample. The oxidized samples were individually stored in a desiccator at room temperature (21 ± 1 °C) between measurements.

XPS. The XPS spectra were obtained using a Quantera scanning X-ray multiprobe from Physical Electronics. The monochromatic Al Kα excitation source was operated at 1486.7 eV and 25 W. The source beam size was 100 μm, analyzing an area of 1000 × 500 μm^2 (scanning X-ray beam). The takeoff angle (angle between the sample surface and the analyzer) was 45°, whereas the angle between sample surface and the X-ray beam was 90°. Survey spectra were obtained at a pass energy of 280 eV. The spectra were referenced to the Si(2p) peak at 101.8 eV.[32] Charge neutralization was achieved by low-energy electrons and low-energy argon ions. The relative error of the surface atomic composition was estimated to be ±5%.

SFM and Tip Modification. The SFM measurements were carried out with a NanoScope III multimode SFM [Digital Instruments (DI), Santa Barbara]. Tapping-mode SFM scans were performed with untreated silicon cantilevers/tips (Nanosensors, Germany) at ambient conditions. 10 and 100 μm^2 *x*- and *y*-range scanners were used. The mean roughness (R_a) was obtained by the evaluation of 0.5 and 1 μm^2 scans according to the procedure described in ref 27a. The surface roughness was measured on at least six different positions on each sample.

Gold-coated triangular-shaped silicon nitride cantilevers and tips (DI) were functionalized using 11-mercapto-1-undecanol by immersion in a 1 mM solution using ethanol as the solvent during 10−40 h, as discussed previously.[27] The functionalized tips were kept in the solutions between measurements and were rinsed in ethanol and dried in a stream of nitrogen immediately before use. Cantilever spring constants were individually calibrated by the thermal noise method.[33] The obtained spring constants ranged between 0.16 ± 0.03 to 0.33 ± 0.05 N m^{-1}. In total, five tips were used. The same tip was used during each set of measurements (at a given exposure and recovery time). For laterally resolved pull-off force measurements, the SFM was operated in the FV mode using a 10 μm^2 *x*- and *y*-range scanner. All FV measurements were performed in Milli-Q water using a liquid cell (DI). Arrays of 64 × 64 $points^2$ (4096 consecutive force−distance measurements) were acquired on at least seven different locations on each sample, using scan sizes of 0.5 × 0.5 μm^2 or 1.0 × 1.0 μm^2. The maximum load applied to the samples was 2 ± 1.5 nN. A custom-built Labview application (National Instruments) was used for signal acquisition and processing. The deflection of the cantilevers was calibrated prior to the measurements by pressing the tip against a hard silicon surface. The raw FV data were transformed into force−distance data using the customized Labview application and the calibrated spring constant. For each force−distance curve, the pull-off force or maximum adhesive force was calculated using an automated procedure. As a result, histograms of adhesion forces were obtained. The slope of the initial unloading curves was used to probe the changes in the

(25) Vezenov, D. V.; Zhuk, A. V.; Whitesides, G. M.; Lieber, C. M. *J. Am. Chem. Soc.* **2002**, *124*, 10578.

(26) Feldmann, K.; Tervoort, T.; Smith, P.; Spencer, N. D. *Langmuir* **1998**, *14*, 372.

(27) (a) Schönherr, H.; Hruska, Z.; Vancso, G. J. *Macromolecules* **1998**, *31*, 3679. (b) Schönherr, H.; Vancso, G. J. *J. Polym. Sci., Part B: Polym. Phys.* **1998**, *36*, 2483.

(28) Trifonova, D.; Schönherr, H.; van der Does, L.; Janssen, P. J. P.; Noordermeer, J. W. M.; Vancso, G. J. *Rubber Chem. Technol.* **1999**, *72*, 862.

(29) (a) Schönherr, H.; Hruska, Z.; Vancso, G. J. *Macromolecules* **2000**, *33*, 4532. (b) Schönherr, H.; van Os, M. T.; Hruska, Z.; Kurdi, J.; Förch, R.; Arefi-Khonsari, F.; Knoll, W.; Vancso, G. J. *J. Chem. Soc., Chem. Commun.* **2000**, 1303. (c) Schönherr, H.; van Os, M. T.; Förch, R.; Timmons, R. B.; Knoll, W.; Vancso, G. J. *Chem. Mater.* **2000**, *12*, 3689.

(30) The PDMS network is formed by a hydrosilylation reaction between vinyl-terminated oligomeric dimethylsiloxanes and a methylhydrosiloxane using a platinum complex as the catalyst.

(31) Garbassi, F.; Morra, M.; Occhiello, E. *Polymer Surfaces. From Physics to Technology*; J. Wiley & Sons, Ltd.: West Sussex, U.K., 1994.

(32) Beamson, G.; Briggs, D. High Resolution XPS of Organic Polymers. *The Scienta ESCA300 Database*; J. Wiley & Sons, Ltd.: New York, 1992.

(33) (a) Hutter, J. L.; Bechhoefer, J. *Rev. Sci. Instrum.* **1993**, *64*, 1868. (b) Gibson, C. T.; Watson, G. S.; Myhra, S. *Scanning* **1997**, *19*, 564.

Table 1. Atomic Surface Composition of UV/ Ozone-Exposed PDMS According to XPS

exposure time (min)	atomic composition (atom %)		
	Si	C	O
0	24.3	44.9	30.8
10	24.5	46.2	29.3
30	24.2	37.3	38.5
60	25.6	20.9	53.5

elastic modulus, according to procedures described previously.[34] The peak value and the width of the histograms were obtained by fitting a Gaussian distribution to the data. For FV imaging, only subsequent up and down scans that showed the same force characteristics were considered.

Result and Discussion

Effects of UV/Ozone Exposure Time. The effect of the UV/ozone treatment time[35] on the atomic surface composition of PDMS was assessed by XPS as summarized in Table 1. Because the atomic surface composition of PDMS may change significantly with the recovery time after exposure to plasmas and corona discharges (the carbon content increases and the oxygen content decreases),[6e] all samples were simultaneously analyzed by XPS within 6 h after UV/ozone exposure. The theoretical atomic composition of PDMS, based on the repeating unit, is 25% Si, 25% O and 50% C. The higher content of oxygen on the expense of carbon found for the unexposed PDMS, compared to the theoretical composition, may suggest a contribution from the silica filler, even though previous studies of silica-filled PDMS led to the conclusion that the silica filler is rarely observed in the probed depth by XPS (∼7−10 nm).[6c,38] When exposed to UV/ozone, the carbon content decreased, whereas the oxygen content increased with increasing exposure time. The silicon content remained constant between 24 and 26 atom % because silicon does not form species that are volatile at room temperature.[8c] The data suggests an increase in the average number of oxygens bonded to silicon, on the expense of the carbon content, that is, oxidative cross-linking within the probed depth. The degree of oxidation was significantly higher between 30 and 60 min of exposure, compared to the initial 30 min. It is suggested that the lower initial oxidation rate was correlated to the time for the UV/ozone cleaner to reach the steady-state concentration of ozone when starting the exposure. High-resolution spectra for the Si(2p) orbital peaks (not shown) showed a broadening and a shift toward higher binding energies at 103.5−103.8 eV, corresponding to the formation of a silica-like structure (SiO_x, $1 \leq x \leq 2$).[32] The high-resolution spectra, in combination with the atomic surface composition presented in Table 1, moreover show that a full conversion into SiO_2 did not occur. The conversion process may be limited by imperfect domains in the converted layers[8c] or migration of free siloxanes into the oxidized region.[6b] A lower conversion can also be an effect of underlying unconverted PDMS contributing to the signal, if the thickness of the SiO_x layer is smaller than the effective sampling depth of XPS.[6b,c] In conclusion, the XPS data indicate the gradual formation of a SiO_x layer with increasing UV/ozone exposure time.[8]

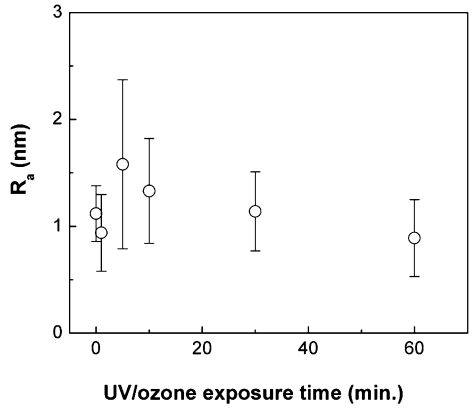

Figure 1. Surface roughness (R_a) as function of UV/ozone exposure time measured by tapping-mode SFM. The error bars indicate the standard deviation.

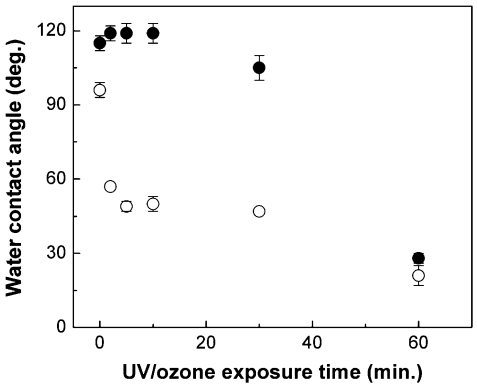

Figure 2. Effect of UV/ozone exposure time on hydrophobicity: ●, advancing contact angles; ○, receding contact angles. The error bars indicate the standard deviation.

Tapping-mode SFM revealed that the exposed PDMS surfaces were smooth, homogeneous, and featureless. The mean roughness (R_a) was not significantly influenced by the UV/ozone exposure (Figure 1).

The effect of the UV/ozone exposure on the hydrophobicity was assessed by water contact-angle measurements (Figure 2). Exposure times below 30 min caused a rapid reduction in the receding contact angles from 103 ± 2° to 45−50 ± 3°, whereas the advancing angles remained essentially unchanged. Because the advancing angles are more associated with the low surface energy regions and the receding angles are associated with the high surface energy regions on heterogeneous polymer surfaces,[6a,36] the unchanged advancing angles indicate that the surfaces were only partly oxidized. The difference between the advancing and the receding contact angle is referred to as the *contact-angle hysteresis* and depends on the roughness, heterogeneity, and molecular mobility (reorientation of functional groups) in the probed surface region.[37] Because the surface roughness was essentially unchanged, the increased contact-angle hysteresis after 2−30 min of exposure suggests the introduction of polar groups (e.g., −OH),[38] which have the possibility of reorienting, depending on the surrounding medium (water or air). PDMS surfaces exposed to 60 min UV/ozone were hydrophilic with advancing and receding contact angles of 28 ± 2° and 21 ± 4°, respectively. The low contact-angle hysteresis indicated a reduced molecular mobility in the surface region compared to the unexposed and partially oxidized surfaces. Efimenko et al. reported recently a similar nonmonotonic time dependence of the contact-

(34) Chizhik, S. A.; Huang, Z.; Gorbunov, V. V.; Myshkin, N. K.; Tsukruk, V. V. *Langmuir* **1998**, *14*, 2606.

(35) We used a combination of UV/ozone because of the lower oxidation rate compared to that of plasmas,[38] making it more suitable for the study of the initial stages of surface oxidation.

(36) Drelich, J.; Miller, J. D.; Good, R. J. *J. Colloid Interface Sci.* **1996**, *179*, 37.

(37) (a) Wu, S. *Polymer Interfaces and Adhesion*; Marcel Dekker, Inc.: New York, 1982; p 25. (b) Yasuda, H. *Plasma Polymerization*; Academic Press: Orlando, 1985.

(38) Efimenko, K.; Wallace, W. E.; Genzer, J. *J. Colloid Interface Sci.* **2002**, *254*, 306.

Table 2. Peak Values and fwhm of the Pull-Off Force Histograms Fitted with a Gaussian Distribution Function Obtained for Hydroxyl-Terminated Tips and Oxidized PDMS Surfaces in Water

UV/ozone exposure time (min)	time after exposure (days)	pull-off force ± σ^a (nN)	fwhm ± σ^a (nN)
unexposed		18.9 ± 1.5	1.5 ± 0.2
10	0.1	5.0 ± 0.1	0.7 ± 0.1
10	50	14.3 ± 1.3	1.5± 0.2
30	0.1	4.2 ± 0.1	0.8 ± 0.1
30	8	13.7 ± 1.4	2.6 ± 0.1
30	50	11.1 ± 1.0	3.8 ± 0.2
60	0.1	2.7 ± 0.3	1.8 ± 0.1
60	8	2.8 ± 0.3	1.7 ± 0.1
60	40	3.0 and 5.5[b]	

[a] Standard deviation. [b] Only the peak values of the bimodal distribution are given.

angle hysteresis when exposing PDMS to UV/ozone.[38] The initial increase in hysteresis was contributed to surface damage caused by chain scission reactions, resulting in a higher degree of surface mobility, whereas the reduced hysteresis at longer exposure times (>60 min) was explained by the formation of a cross-linked silica-like structure. While XPS and contact-angle measurements provide laterally resolved data on a continuum scale, CFM was utilized to obtain complementary information of the nanometer scale.

When performing CFM, the surface roughness can easily interfere with the evaluation of the force measurements because the pull-off force depends on the contact area between the tip and the sample.[27,39] Because the roughness was low for all the investigated samples (R_a < 2 nm), only a minor influence of the sample topography on the force measurements was expected.[27,39] Forces between hydroxyl-terminated SFM tips and the PDMS surfaces were characterized by SFM force−distance curves. All measurements were performed in water to avoid the appearance of a meniscus between the tip and the surface by adsorbed water, which gives rise to uncontrolled capillary forces.[39b,40] The attractive force (pull-off force) in the unloading part of the force−distance curves reflects the adhesion between the tip and the surface. It has previously been shown that solvent exclusion forces dominate the interaction between hydrophobic tips (methyl-terminated or even contaminated unmodified tips) and hydrophobic surfaces.[18a,27,25] In this study, hydroxyl-terminated tips were used, thereby reducing the pull-off forces from ∼150 nN (unmodified tips) to 19 nN on unexposed PDMS surfaces. The adhesion mapping comprised 4096 consecutive force−distance curves, generating a two-dimensional image of the pull-off forces with a sub-50-nm resolution.[41] The mean pull-off forces and the full width at half-maximum (fwhm) were then estimated from the corresponding pull-off force histograms by fitting Gaussian distributions. Mean pull-off forces and the fwhm's acquired from all images are summarized in Table 2. Thus, each reported pull-off force value is based on at least 28 672 (7 × 4096) pull-off events.

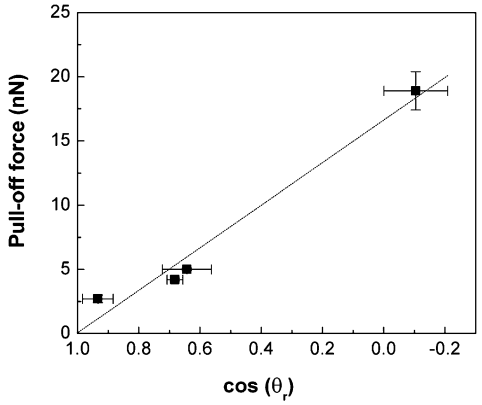

Figure 3. Pull-off force as a function of the cosine of the receding contact angle (θ_r) directly after 0−60 min of UV/ozone exposure. The line is added as guidance for the eye.

For unexposed PDMS, a mean pull-off force of 18.9 ± 1.5 nN was obtained. Exposure to 10 and 30 min of UV/ozone exposure resulted in a reduction in the pull-off forces down to 5.0 ± 0.1 and 2.7 ± 0.3 nN directly after exposure, respectively. The major reduction in the pull-off forces thus occurred within the first 10 min of exposure. The reduction in the mean pull-off force is a result of decreasing solvent exclusion forces between the hydrophilic tip and the gradually more hydrophilic surfaces in water.[18a] The corresponding adhesion images (not shown) were homogeneous and featureless, indicating a homogeneous oxidation on a sub-50-nm level. This homogeneity was also reflected in a reduced fwhm of the pull-off force histograms. After 60 min of exposure, regions with diameters <50 nm with higher adhesion (4−6 nN) were observed, indicating inhomogenieties in the oxidized surfaces (see Figure 8b, where the arrow indicate areas with higher pull-off forces). In Figure 3, the pull-off forces of the PDMS surfaces directly after exposure to 0−60 min UV/ozone are plotted as a function of the cosine of the corresponding receding water contact angles.[42] A linear relationship was observed, which is in agreement with data obtained by Schönherr et al.[27,29a] This shows that contact-angle measurements and average pull-off forces by SFM using functionalized tips provide similar information for polymers. However, by using position-resolved force measurements one can take full advantage of the high-resolution *microscopic* nature of the SFM and, thus, obtain novel insight into forces and, indirectly, hydrophobicity on a nanometer scale.

The slopes of the initial unloading curves were used to probe changes in the elastic modulus after UV/ozone exposure. The thus estimated modulus of unexposed PDMS was 1.4 ± 0.4 MPa. Recently, Feinberg and Brennan reported an increase in the modulus from 1.5 ± 0.8 to 3.0 ± 0.9 MPa when exposing a cross-linked PDMS to an argon−plasma.[43] In the present study, no attempt was made to calculate the elastic modulus of the oxidized surfaces because the obtained values do not reflect the true modulus of the silica-like layer but may rather be considered as the sum of a laminate structure, with a high modulus surface layer on top of the PDMS elastomer.

(39) (a) Eaton, P. J.; Graham, P.; Smith, J. R.; Smart, J. D.; Nevill, T. G.; Tsibouklis, J. *Langmuir* **2000**, *16*, 7887. (b) Eaton, P. J.; Smith, J. R.; Graham, P.; Smart, J. D.; Nevill, T. G.; Tsibouklis, J. *Langmuir* **2002**, *18*, 3387.

(40) Schenk, M.; Füting, M.; Reichelt, R. *J. Appl. Phys.* **1998**, *84*, 4880.

(41) On the basis of the contact area at the pull-off as described by the Johnson−Kendall−Roberts theory of adhesive contact [Johnson, K. L.; Kendall, K.; Roberts, A. D. *Proc. R. Soc. London, Ser. A* **1971**, *324*, 301. Noy, A.; Frisbie, C. D.; Rozsnyai, L. F.; Wrighton, M. S.; Lieber, C. M. *J. Am. Chem. Soc.* **1995**, *117*, 7943]. Using a scan size of 1 × 1 μm^2 and an array of 64 × 64 measurements, the pixel size is 15.6 nm. The resolution in the presented data is, thus, limited by the area at pull-off.

(42) The receding angles were used because they are more sensitive to the introduction of hydrophilic regions on a hydrophobic surface compared to the advancing contact angles [Wu, S. *Polymer Interfaces and Adhesion*; Marcel Dekker, Inc.: New York, 1982].

(43) Feinberg, A. W.; Brennan, A. B. *Polym. Mater. Sci. Eng.* **2003**, *88*, 574.

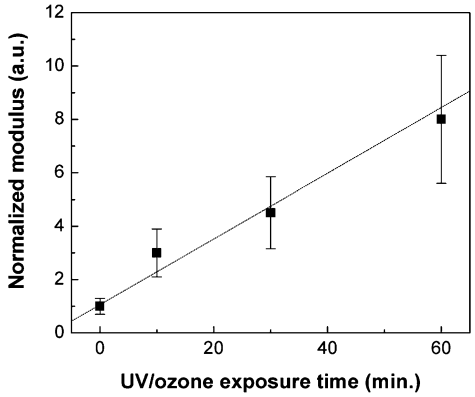

Figure 4. Normalized modulus obtained from indentation mapping by SFM as a function of the UV/ozone exposure time. The normalized modulus of unexposed PDMS = 1. The error bars indicate an estimated error of 30%. The line is added as guidance for the eye.

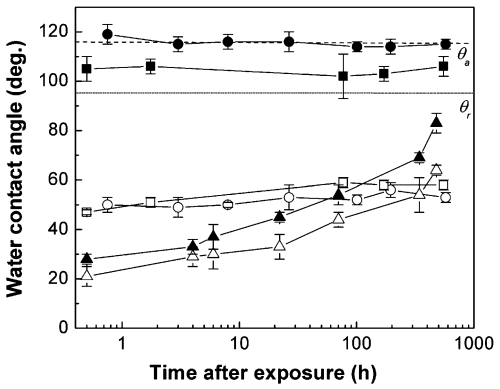

Figure 5. Hydrophobicity as a function of the time after exposure: 10 min of UV/ozone exposure (●, advancing angles; ○, receding angles); 30 min of UV/ozone exposure (■, advancing angles; □, receding angles), and 60 min of UV/ozone exposure (▲, advancing angles; △, receding angles). The error bars indicate the standard deviation. The horizontal lines indicate the initial advancing (θ_a) and receding (θ_r) contact angles, and the continuous lines are added as guidance for the eye.

Instead, the indentation data was normalized with respect to the modulus of the unexposed PDMS. The average normalized modulus, based on the laterally resolved modulus measurements, increased linearly with UV/ozone exposure time, as shown in Figure 4. The featureless appearance of the exposed surfaces by the lateral modulus mapping (not shown) indicated again a homogeneous oxidation on a <50-nm level directly after exposure. The low increase in the modulus, compared to the elastic modulus of SiO_2 (70 GPa)[44] is in agreement with data obtained by specular X-ray reflectivity, where the material density within the first ~5 nm of UV/ozone-exposed Sylgard 184 was found to reach about 50% of that of pure silica.[38] Using the term "silica-like layer" in the sense of "glasslike" may be misleading because the presented data indicate the formation of a surface structure, which differs significantly from that of silica.

Hydrophobic Recovery Probed by Contact-Angle Measurements and CFM. The hydrophobic recovery after 10, 30, and 60 min of UV/ozone exposure was assessed by water contact-angle measurements (Figure 5). No significant change in the hydrophobicity was observed after 10 and 30 min of exposure. After 60 min of exposure, the hydrophobicity, as well as the contact-angle hysteresis, gradually increased with time after exposure (recovery time). This *hydrophobic recovery* is a characteristic behavior of PDMS surfaces after exposure to oxidizing plasmas, as previously discussed in the Introduction. As a result of the different natures of the recovery processes after exposure, we discuss the recovery process in two separate sections.

Hydrophobic Recovery of Partially Oxidized PDMS Surfaces (≤30 min of Exposure). Even though the hydrophobicity remained essentially constant with time after exposure, as measured by the contact-angle measurements, "hydrophobic recovery" occurred on the nanometer scale, as assessed by CFM. The pull-off forces increased from 4 to 5 nN directly after exposure and up to 11−14 nN 8−50 days after exposure (Table 2). The fwhm increased with the storage time, reaching, or in the case of the 30 min exposure exceeding, the initial value of 1.5 nN, while the histograms still remained Gaussian in shape. This broadening suggests an increased inhomogeneity of the probed surface with time after exposure. However, the adhesion mapping (not shown) revealed homogeneous surfaces on the sub-50-nm level. Frequent contamination of the SFM tips occurred during measurements of the recovered surfaces (observed as temporary irreproducible variations in pull-off forces). Thus, the higher mean pull-off forces of the recovered surfaces may be caused by contamination of the hydroxyl-terminated tips. It has previously been shown that low-molar-mass PDMS readily contaminates SFM cantilever tips.[45]

Droplet-shaped features appeared on the surfaces of some of the probed regions.[46] The initial diameters were <30 nm, but they gradually increased in size with the recovery time to sizes on the order a few hundred nanometers (Figure 6a). The maximum adhesive forces of these droplets were of the same magnitude as the surrounding surface (Figure 6b), but the force curves differed significantly in shape (Figure 6d). While the surrounding surfaces exhibited well-defined pull-on and pull-off events, the force curves of the droplets exhibited a more gradual pull-on and a "necking" instead of a distinct pull-off, giving rise to a large adhesion hysteresis (i.e., the area enclosed between the approach and retract curves was higher for these droplets; Figure 6c). This necking instead of a pull-off is caused by a viscoelastic flow between the oxidized PDMS and the SFM tip and has been attributed to interactions between free oligomeric PDMS and the tip.[43,47] It may be speculated that the "droplike" structures are caused by a gradual coalescence of low-molar-mass siloxanes, generated by chain scission reactions during exposure, which strive to assume spherical shapes to minimize the surface free energy. This is based on the assumption that these free siloxanes exhibit a lower degree of oxidation at the surface, thereby having a lower surface free energy.

Also, the normalized modulus recovered with time after exposure, approaching the value of unexposed PDMS (Figure 7). The recovery was more pronounced after 30 min of exposure, compared to 10 min. The asymmetric shape of the distributions toward the higher modulus was maintained during the recovery process even though the width of the distributions decreased. After 40−50 days of

(44) Kayne, G. W. C.; Laby, T. H. *Tables of Physical and Chemical Constants*; Longman: Essex, U.K., 1985.

(45) Lo, Y. S.; Huefner, N. D.; Chan, W. S.; Dryden, P.; Hagenhoff, B.; Beebe, T. P., Jr. *Langmuir* **1999**, *15*, 6522.

(46) These droplets were also characterized using tapping-mode SFM. By decreasing the set point (e.g., increase the applied peak force), these droplets could no longer be visualized, indicating that they were liquidlike in nature (likely free siloxanes), thereby allowing the tip to penetrate down to the surface.

(47) Pickering, J. P. Ph.D. Thesis, University of Twente, Enschede, The Netherlands, 2001.

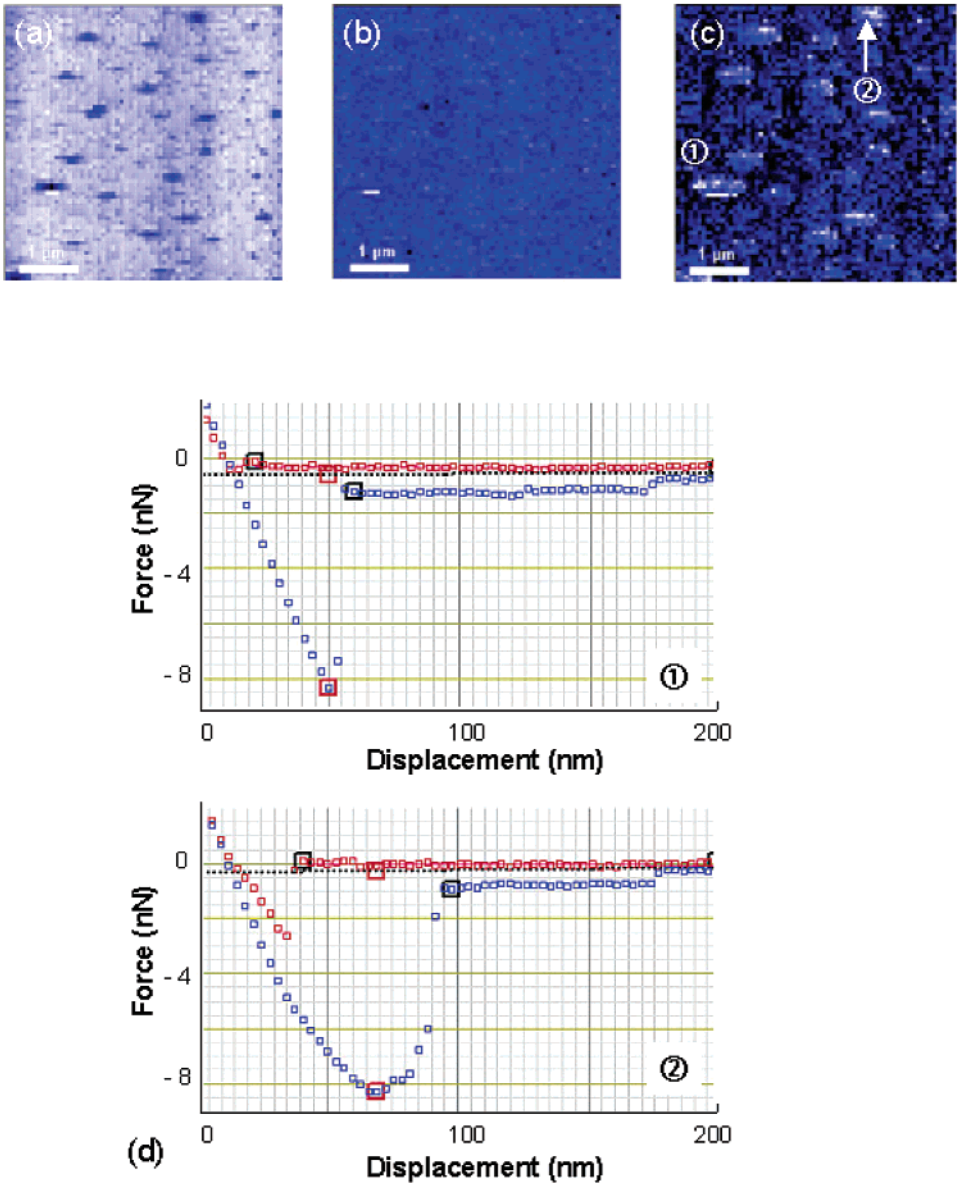

Figure 6. CFM of "droplets" appearing with time after 30 min of UV/ozone exposure: (a) height, (b) maximum adhesive forces, and (c) adhesion hysteresis. The color scales indicate the *height* [bright (0 nm) to dark (10 nm]; *maximum adhesive force* [dark (6 nN) to bright (l7 nN)]; and *hysteresis* [dark (0.2×10^{-17} J) to bright (1.2×10^{-17} J)]. (d) Representative force−distance curves.

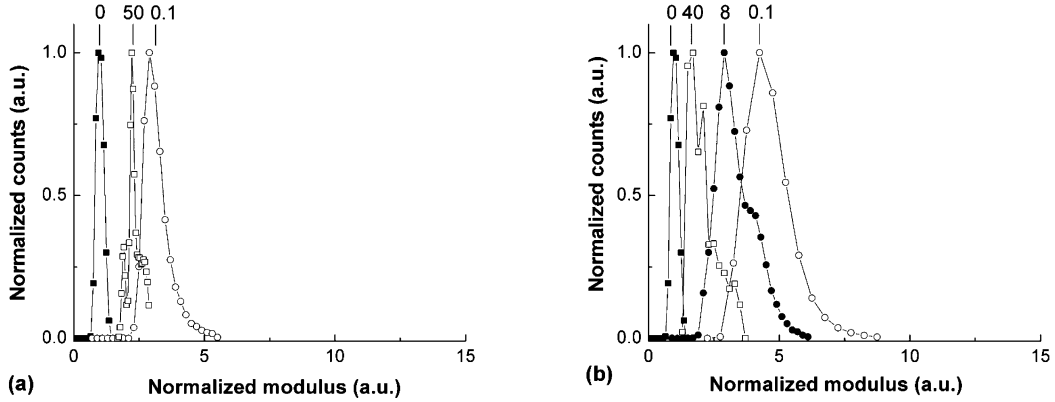

Figure 7. Effect of the recovery time on the normalized modulus obtained from SFM indentation mapping after (a) 10 and (b) 30 min of UV/ozone. Recovery times in days are indicated above the distributions. The peak indicated by 0 corresponds to unexposed PDMS (normalized modulus = 1).

recovery, the normalized modulus of the oxidized surfaces had reached a similar value, approximately 1.5−2 times higher than the value of unexposed PDMS.

The fast recovery of pull-off forces, the gradually decreasing modulus, and the featureless appearance of the surfaces during CFM mapping, in combination with

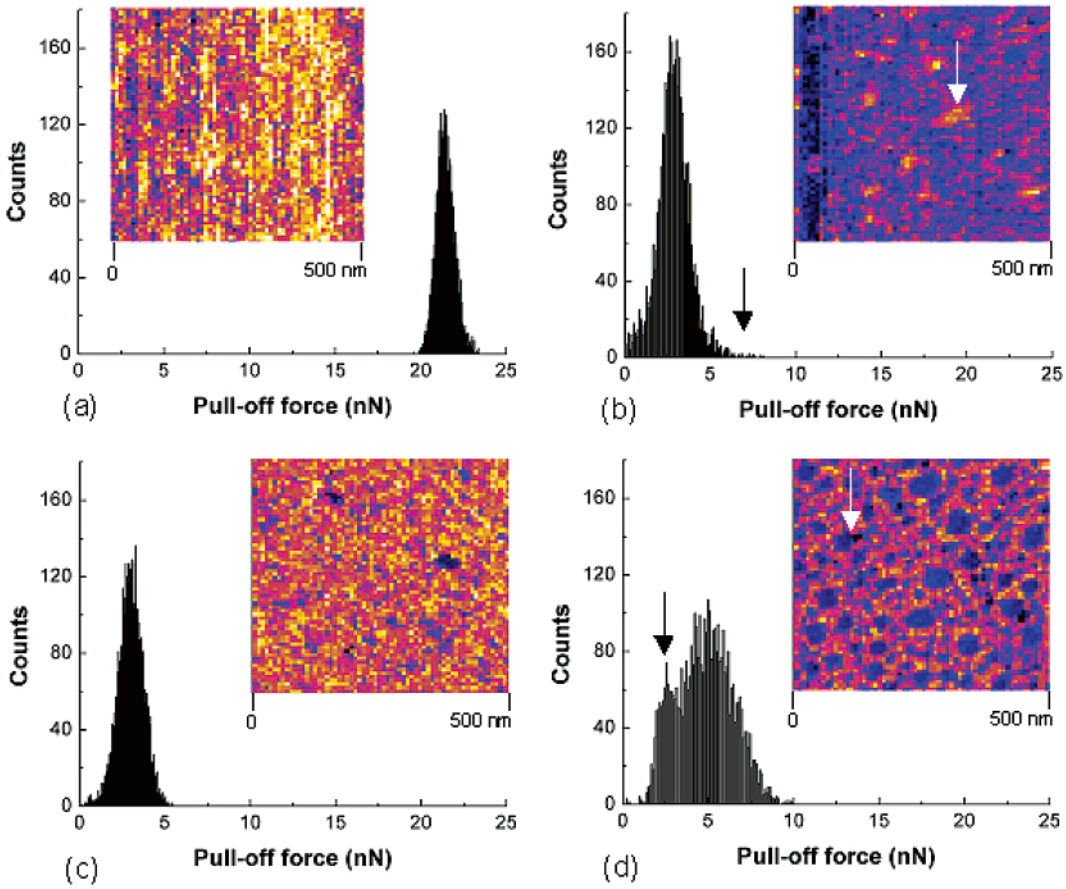

Figure 8. Representative histograms of the pull-off forces and corresponding adhesion images of (a) unexposed PDMS and oxidized PDMS after (b) 0.1, (c) 8, and (d) 40 days after exposure to 60 min of UV/ozone. In the adhesion images, the color scales are individually scaled from dark (low pull-off) to bright (high pull-off).

the contact-angle data, can be explained by a gradual formation of a liquidlike layer consisting of oligomeric, free PDMS on top of the partly oxidized PDMS surface after exposure. These free siloxanes may be formed by chain scission reactions during UV/ozone exposure, or they may be present in the bulk. The XPS data, which have a higher penetration depth compared to the CFM, suggest a partial conversion into SiO_x. The oxidized surface is, thus, gradually masked by the siloxanes and may hide eventual surface heterogeneities. The decrease of the normalized modulus with the aging time also indicates an enrichment of free siloxanes in the probed region, which can be considered as a sum of the unexposed bulk and an oxidized surface region of unknown thickness partially or fully covered by a liquidlike layer.

Hydrophobic Recovery of Silica-like Surface Layers (60 min of Exposure). After 60 min of UV/ozone exposure, the initially hydrophilic surface gradually recovered hydrophobicity, as assessed by the water contact-angle measurements (Figure 5). A full recovery was not obtained during the course of the experiment. The "hydrophobic recovery" of the mean pull-off forces was significantly lower, compared to 10 and 30 min of UV/ozone-treated samples, and did not reach above 5 nN (Table 2). Moreover, the force−distance curves exhibited well-defined pull-off events. The adhesion mapping revealed that the surface gradually increased in heterogeneity with recovery time, a phenomenon that was not observed after the shorter exposure times. This trend is illustrated in Figure 8, where representative pull-off distributions are shown together with the corresponding pull-off images. A bimodal distribution of the pull-off forces developed with the recovery time with the appearance of an additional peak at 5−6 nN. The adhesion mapping showed that the bimodal shape of the pull-off distributions was a result of the appearance of domains with a diameter of <100 nm and heights of <5 nm, which exhibited lower pull-off forces ($\sim$3 nN), whereas the surrounding areas exhibited higher surface pull-off forces (5−6 nN). One typical region with low pull-off forces is indicated with an arrow in Figure 8d.

The surface modulus decreased with time after exposure, even though the decrease is significantly lower compared to the shorter exposure time (Figure 9a). Furthermore, the asymmetric shape of the distribution toward a higher modulus was maintained during the recovery. The modulus mapping showed that the areas with a higher normalized modulus corresponded to the domains with lower pull-off forces (see Figures 9b and 8d).

On the basis of these observations, we attribute the stiffer regions with a pull-off force of 3 nN (as measured 40 days after exposure) as SiO_x-rich areas. These regions, which may be only partially covered with PDMS, are, hence, similar to the freshly oxidized PDMS surface directly after exposure. Consequently, the surrounding areas must have gradually decreased in modulus. It is suggested that the increased heterogeneity is driven by a difference in the interfacial energies between polar and nonpolar species generated during the exposure and some rearrangement in the surface-near region of the samples. An additional mechanism may be driven by strain release. When the surface undergoes a transition to a new inorganic species, strain is created between more and less converted regions.[9] Relaxation of these stresses between more and less cross-linked regions may then contribute to the observed structure. These processes may be aided

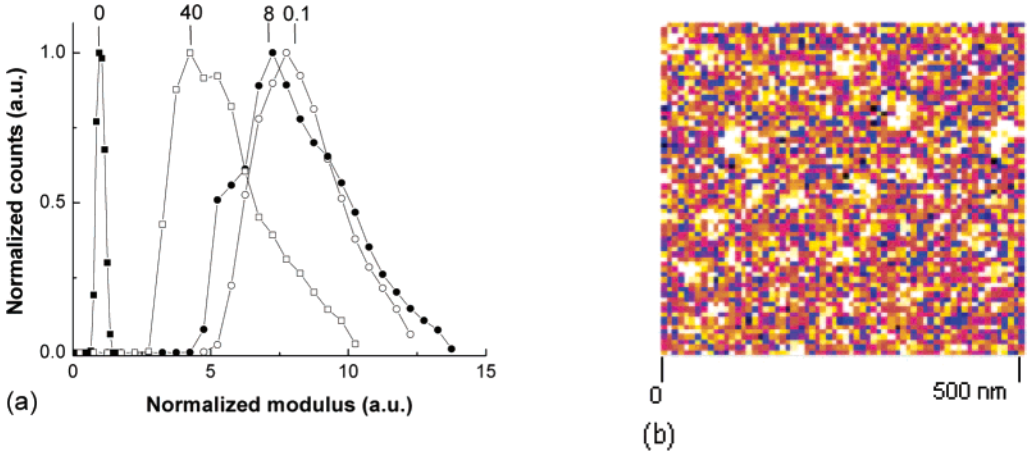

Figure 9. (a) Effect of the recovery time on the normalized modulus obtained from SFM indentation mapping, after 60 min of UV/ozone. Recovery times in days are indicated above the distributions. The peak indicated by 0 corresponds to unexposed PDMS (normalized modulus = 1). (b) Example of modulus mapping, 40 days after 60 min of UV/ozone; the color scale corresponds to a normalized modulus from 2 (dark) to 10 (bright).

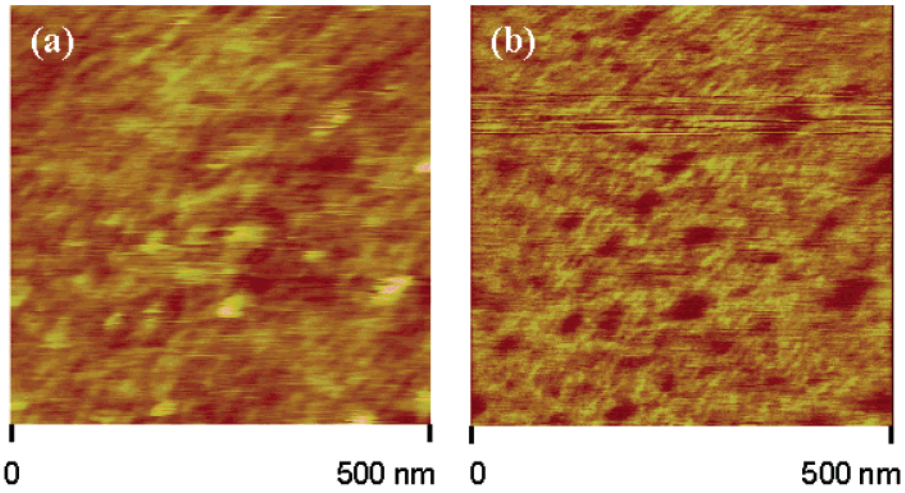

Figure 10. Contact-mode SFM of oxidized PDMS in water using a hydroxyl-terminated tip. Analysis 40 days after exposure to 60 min UV/ozone: (a) height image, *z* scale = 0−10 nm, (b) friction image [friction forces (arbitrary units) increase from a dark to a bright contrast].

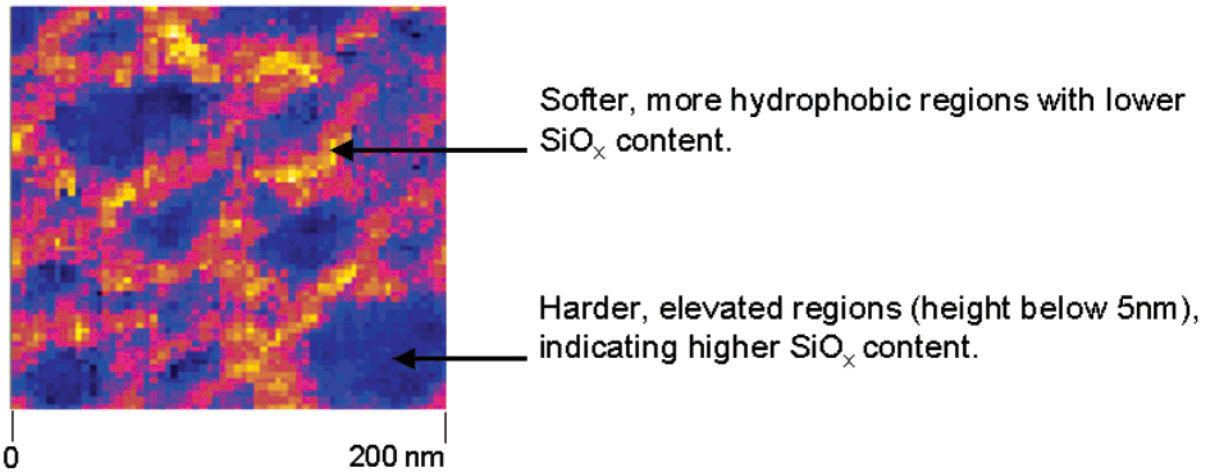

Figure 11. Illustration of the spatial structure of a silica-like layer in equilibrium by adhesion mapping, 40 days after 60 min of UV/ozone exposure. The color scale corresponds to pull-off forces from 0.2 nN (dark) to 4 nN (bright).

by the increased mobility, caused by chain scission reactions.[48] The structures observed after 40 days of recovery remained unchanged when the same sample was analyzed again seven months later, indicating that an equilibrium was reached and that this was the final stable structure of a silica-like surface layer. These surface structures were also imaged in contact-mode SFM, using

(48) No problems with tip contamination occurred during the measurements of these surfaces, as frequently occurred on surfaces exposed to 10 and 30 min of UV/ozone exposure.

hydroxyl-terminated tips in water, to verity the data obtained by the adhesion mapping (Figure 10). The elevated areas exhibited heights below 5 nm and a lower friction compared to the surrounding matrix. This is in agreement with stiffer hydrophilic elevated domains surrounded by a softer, less hydrophilic matrix. This structure is summarized in Figure 11, showing an adhesion image of oxidized PDMS 40 days after 60 min of UV/ozone exposure.

Conclusions

CFM in water was used to map the surface hydrophobicity on UV/ozone-treated PDMS (Sylgard 184) and to follow its changes as a function of storage/aging time. In addition to CFM pull-off force mapping, we applied indentation mapping to probe the changes in the normalized modulus. These experiments were complemented by results on surface properties assessed on the micrometer scale by XPS and water contact-angle measurements. UV/ozone exposure times shorter than 30 min resulted in oxidized surfaces with a high segmental mobility, reflected in relatively hydrophobic surfaces exhibiting a high water contact-angle hysteresis. SFM pull-off force and indentation measurements revealed the formation of a homogeneous (on a <50-nm scale), hydrophilic surface with an increased normalized surface modulus directly after exposure. The subsequent "hydrophobic recovery" was characterized by a gradual increase in the pull-off forces, toward the initial values, in combination with a decrease in the normalized modulus to 2 times the original value. Lateral imaging showed the appearance of liquid PDMS, in the form of droplets (ranging from 30 nm to several micrometers in size) with increasing recovery time. By contrast, longer UV/ozone exposure times (60 min) led to the formation of a hydrophilic silica-like structure, as assessed by XPS and water contact-angle measurements, which exhibited a slow and incomplete hydrophobic recovery. CFM pull-off force and stiffness mapping revealed a laterally heterogeneous, high modulus surface with <50-nm features with higher hydrophobicity (higher pull-off forces) directly after exposure. A gradual surface reconstruction within the silica-like layer occurred with time after exposure, where a hydrophilic SiO_x-enriched phase formed <100-nm sized domains, surrounded by a more hydrophobic matrix with a lower normalized modulus.

Acknowledgment. The authors gratefully acknowledge financial support from the Swedish Foundation for International Cooperation in Research and Higher Education in the form of a postdoctoral scholarship (PD 2001-237; H.H.), the Dutch Polymer Institute (DPI) (A.O.), and the Council for Chemical Sciences of The Netherlands Organization for Scientific Research (CW-NWO; H.S. and N.T.).

LA035552K